Improved estimation of forest carbon (biomass) using bi-temporal RapidEye data in a low-altitude tropical landscape

[1] **Glen R. Yali,** [2] **Sailesh Samanta and** [3] **Cossey K. Yosi**

[1, 2] *Department of Surveying and Land Studies, Papua New Guinea University of Technology, Private Mail Bag, Lae 411, Morobe Province, Papua New Guinea*
[3] *Papua New Guinea Forest Research Institute, P O Box 314, Lae 411, Morobe Province, Papua New Guinea*

[1] *yaliglenn@gmail.com,* [2] *rsgis.sailesh@gmail.com,* [3] *cyosi@fri.pngfa.gov.pg*

Abstract

In the recent past, optical satellite data have been widely used in estimating forest parameters, particularly above-ground biomass (AGB) and carbon (C) stocks, but were not used much in Papua New Guinea (PNG) forest studies. In this study, forest inventories conducted in 2009 and 2014 for ground estimation of AGB and C were linked with bi-temporal high resolution (5m) optical RapidEye satellite data for 2010 and 2014respectively for estimation at spatial levels using an improved strategy in a low-altitude tropical landscape of PNG. In order to improve the overall estimation process, specific spectral indices were derived from the Red band of the RapidEye data along with explorative derivation of such using the Red Edge narrow-bandto act as added variables for correlation with AGB and C. Variable appropriation for the modeling found significance in the Red Edge derived spectral indices over those derived normally from the Red band. Using these spectral parameters, single preeminent variables were identified and utilized to model AGB and C in each forest stratum via a spatial linear regression analysis. This study presents the idea of generating stratum-specific models using RapidEye imageries and merging these models through the notion of model-fitting for effective cross-landscape estimation of C stocks. The two broad forest stratums analysed were undisturbed primary forest (PF) and disturbed secondary forest (SF). Stratum-specific models developed for PF and SF using spectral indices had high confidence levels of $p < 0.01$ for both PF and SF in 2010 and also sound confidence levels of $p < 0.05$ for both PF and SF in 2014. The overall root mean square errors (RMSEs) for both temporal models were reasonably low with values $<9MgC\ ha^{-1}$ and $<29MgC\ ha^{-1}$ across the study area. RMSEs for the model-fitswere attuned and more promising with values $< 7MgC\ ha^{-1}$ and $< 18MgC\ ha^{-1}$ respectively.These results show that the strategy of stratum-specific modeling used here is an effective approach that can be well applied in other low-altitude tropical forest landscapes in PNG with high resolution optical satellite data for efficient C stock estimations for REDD+ implementations.

Keywords: *AGB, C, RapidEye, spectral indices, stratum-specific models, temporal.*

1. Introduction

According to the JICA (Japan International Corporation Agency) – PNGFA (Papua New Guinea Forest Authority) Project for Capacity Development on Forest Monitoring for Addressing Climate Change(The National, 2014, March 13), AGB and C dynamics monitoring at vast scales are currently analysed using high resolution RapidEye satellite data as an improved optical remote sensing product together with active microwave remotely sensed Radar (Phased Array type L-band Synthetic Aperture Radar onboard Advanced Land Observation Satellite – ALOS PALSAR) (Rosenqvist *et al*., 2007) data across PNG. These remote sensing data are also being used solely to map and monitor PNG forests. Thus, since RapidEye data is currently used by the Papua New Guinea Forest Research Institute (PNGFRI) under the PNGFA to map and monitor forest parameters at a national level, its usage in this study is relevant. The UNREDD/REDD+ (UNFCCC, 2009 & 2010) are currently focused on forests in the tropics (Bryan *et al*., 2011) and because PNG has the largest tropical rainforest in the South Pacific region (Sharman *et al*., 2008), the estimation of sequestered (stored) C stocks via improved strategies of space-borne (satellite) approaches are the effective means needed for large-scale carbon estimation.

Regarding space-borne approaches, Wijaya*et al*. (2010a) used certain specific spectral indices such as complex vegetation indices with simple ratio indices derived from medium resolution optical Landsat 7 ETM+ (Enhanced Thematic Mapper Plus) satellite data to analyse relationships with AGB and C in tropical Indonesian forests and found that complex Global Environment Monitoring Index (GEMI)(Pinty and Vestraete, 1991) was a preeminent variable in their AGB and C estimation model. Eckert (2012) also explored the relationship of specific spectral indices involving complex vegetation indices and simple ratio indices from high resolution optical WorldView-2 satellite data with AGB and C and found model significance in complex Enhanced Vegetation Index (EVI) (Huete *et al*., 1997). Accordingly, such specific spectral indices were used in this study to analyse relationships with AGB and C for their subsequent modeling and estimation.Linear regression approaches have been widely applied for prediction of AGB and C using spectral parameters from optical remote sensing data (Eckert, 2012; Hall *et al*., 2006; Rahman *et al*., 2008; Wijaya *et al*., 2010a & b; Zheng*et al*., 2004) and were also applied in the present study to develop estimation models for AGB and C. The initial study done (Yali and Samanta, 2014) was, however, only limited to the relationships between simple spectral reflectance (single image bands) from Landsat 7 ETM+ data with AGB and C for the estimation at spatial levels in a lowland forest.

The aim of this study is to integrate ground estimates of AGB and C with spectral parameters of the RapidEye imageries to analyse their relationship and the potential of RapidEye data to improve estimation of AGB and C for two tropical forest stratums on a bi-temporal platform. The study objectives, therefore, are (i) to derive appropriate variables for AGB and C modeling, (ii) to develop stratum-specific models for improved estimation of AGB and C and via model-fitting, demonstrate spatially distributed estimates of C. Notably, the overall estimation process in this study from ground estimates to correlation and finally to modeling will refer to both AGB and C hereafter despite the focus on C stocks because forest biophysical features observable by satellite sensors are directly related to AGB and C is only a vital sequestered constituent of AGB.

Conjecture-wise this study hypothesizes that explorative derivation of the spectral indices from the RapidEye's Red Edge narrow-band will assume significance in their correlation with AGB and C.

Also, since this study uses bi-temporal RapidEye data to develop stratum-specific models (Eckert, 2012) it hypothesizes the idea of model-fitting as a good strategy for validating the integration of these models in the spatial domain for temporal cross-landscape estimation.
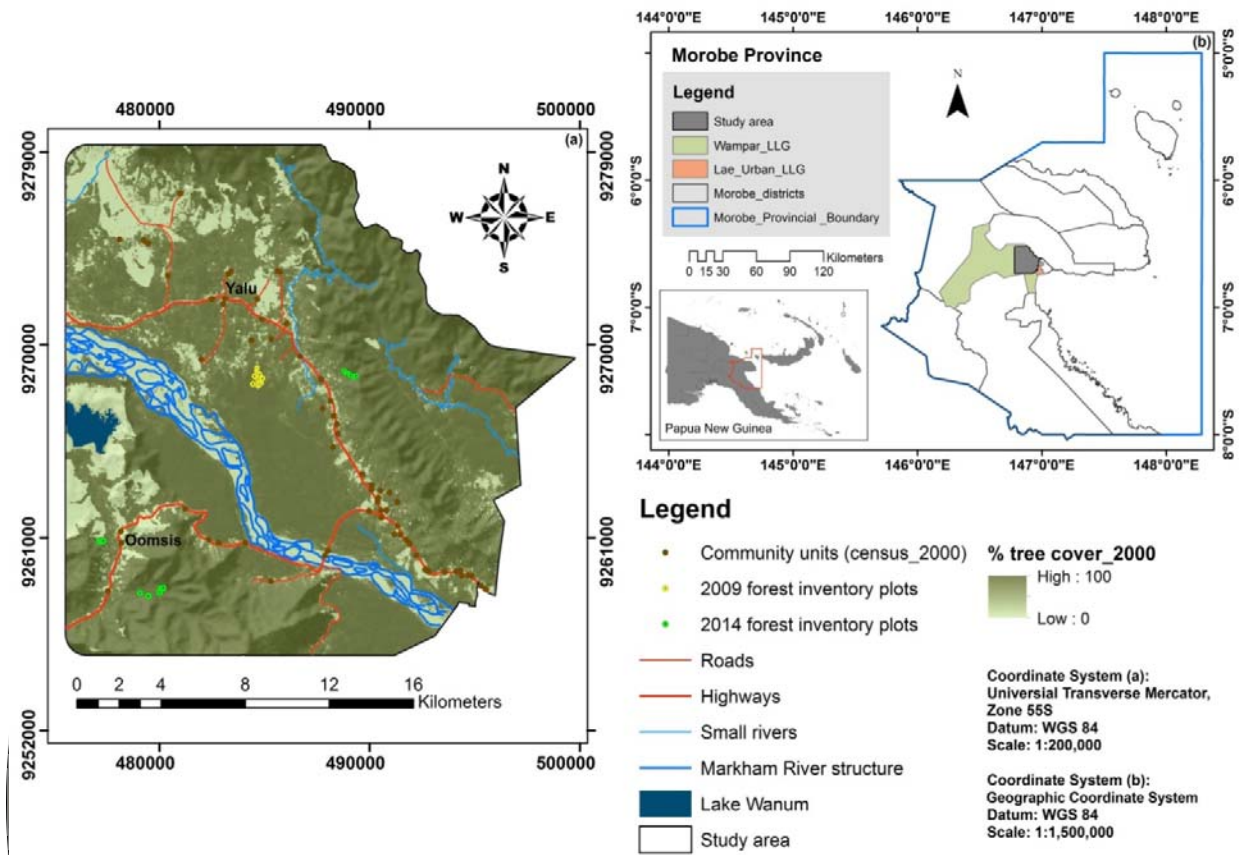
2. Study Area

The study area is situated in the western part of the central region of Wampar Local Level Government(LLG) in the Huon District of Morobe Province, PNG. It lies approximately 8 km precisely northwest of Lae City and shares a common boundary with Lae Urban LLG (see Figure 1).Its geographical extent from north to south is 146° 50' 24" E, 6° 31' 12" S to 146° 50' 24" E, 6° 44' 24" S and its entire extent was defined according to the scene extent of the acquired RapidEye imageries. The study area has a total annual precipitation of 2336 millimetres (mm) and falls within a regional annual temperature range of 22 to 34°C.It also has major forest areas in the north-eastern and south-western parts where there is high elevation. Elevation peaks range from 150 to 1000m above sea level.The study area also contains the junction of the two major highways in Morobe Province and according to Figure 1 the highway extending north-west to west is the Highlands (Okuk) Highway, while the other extending west to south-west is the Bulolo Highway. Figure 1 also shows the location of the study area and gives a historical depiction of the forest cover for Year 2000 captured by Landsat7 ETM+ sensor and measured in percentage (%).

The study area has the most sensitive forest in the whole of Wampar LLG as it is highly subjected to mainly agricultural land-uses with substantial forestry activities as well as infrastructure development and other urban development (settlements). The primary vegetation of the study area typically ranges from low-altitude forest on uplands, to low-altitude forest on plains and fans and low-altitude woodland with other less dominant but important lowland forest stratums.

The most dominant tree species identified by the 2009 forest inventory was *Pterocarpusindicus* (Rosewood) with *Celtis* (Celtis) and *Pometiapinnata* (Taun) as the other two common species. In the 2014 forest inventory the dominant species was *Ficus* (Fig) with*Celtis* (Celtis), *Syzygium* (Water Gum), *Myristica* (Nutmeg) and *Cryptocarya* (Cryptocarya) identified as other common species by count. Most but not all species identified in both of the forest inventories were listed as the 50 most common species on the PNGFRI's Permanent Sample Plots (PSP) (Fox *et al.*, 2010).

The two broad forest stratums evaluated for the estimation ofC stocks across the study area were (i) primary forests (PF) consisting of undisturbed forests with mature growths (Fox *et al.*, 2010) and (ii) secondary forests(SF) comprising disturbed forests (Brown & Lugo, 1990) including Riparian (open) forests (Wijaya *et al.*, 2010).

Fig 1. Location map of the study area, a low-altitude landscape portion of central Wampar LLG referencing Morobe Province and PNG and also showing Yalu and Oomsis sample sites

3. Materials and Methods

3.1 *Field Data*

Field estimation of AGB and C stocks for the entire study area involved data collected from two dates, 2009 and 2014. For location of sample plots, two sites were sampled in Yalu and Gabensis respectively in 2009 (Yosi, 2011) whereas in 2014 two sites were sampled in Omsis with one site in Yalu. In Yalu forest, 2009 plots were located on the west of the Highlands Highway while 2014 plots were located on the Atzera Range lying adjacent to the Highlands Highway on the east (see Figure 1). For Oomsis, sample plots were located on the uplands of Oomsis hills with only three plots from those located at the east of Bulolo Highway situated on a subtle low lying plain between the uplands.

The forest sampling method used was *Variable Radius Sampling Technique* (Fox *et al*., 2011a), a modern forest inventory technique also known as *point samples* or *plot-less samples* which was introduced to PNGFA by Australian Centre for International Agricultural Research (ACIAR) in 2003 for application in forest inventories and was also applied in Yosi (2011). Forest in-situ data were collected from 18 sample plots for 2009 and 14 sample plots for 2014 totalling 32 samples for

retrieval of AGB parameters especially diameter at breast-height (DBH).For definition of sample trees a "Wedge" or "Basal Area" Prism radarscope was used to identify unbiased samples within each plot in a clock-wise direction from the plot centres. A hand-held GPS was used to capture the centre location of each plot and plot radius ranged from 10 to 15 meters. Only DBH was measured using π-calibrated diameter tapes for trees that were identified as samples by the Wedge Prism. The measurements comprised trees with diameters >10cm, having matured stand structures.In order to estimate tree heights for each sample tree, a height-diameter (*H-D*) model developed earlier in a collaborative research by the ACIAR and PNGFRI (Fox *et al.*, 2010; Fox *et al.*, 2011a; Fox *et al.*, 2011b) was applied. The equation applied to estimate tree heights is as follows:

$$H = aD \div b + D$$

where, H is the tree height, a and b are parameters estimated from H-D models in PNGFRI's PSPs and D is the diameter (DBH).

AGB and C for sample plots were estimated using Chave*et al.*'s (2005) biomass model, a wet tropical allometry developed from an extensive study of tropical forests including those in PNG and was successfully applied in Fox *et al.* (2010 & 2011a) and Yosi (2011) for PNG low-altitude forests and Yali & Samanta (2014) in a lowland forest landscape. This model takes the form:

$$AGLB = 0.776 \, [\rho D^2 H]^{0.940}$$

where*AGLB* is aboveground live biomass in kilograms (kg), ρ is wood specific gravity (density at 0% moisture) in grams per cubic centimetres (g cm^3),*D* is tree diameter (DBH) in centimetres (cm) and *H* is total tree height in meters (m) (Fox *et al.*, 2010 and Fox *et al.*, 2011). For the estimation of AGLB in this study, the wood density for each tree was obtained from three sources: (i) available wood densities for PNG timber species in Eddowes (1997); (ii) wood densities from compiled work on Asian rainforest by Intergovernmental Panel on Climate Change (IPCC) (2006) and (iii) an overall average wood density value of 0.477g/cm³ across all PNG tree species in PNGFRI's PSPs (Brown, 1997; Chave *et al.* 2003). The C measure of the forest as specified in Fox *et al.* (2010 & 2011a) is 50% of the dry (0% moisture) biomass (Clark *et al.*, 2001; Houghton *et al.*, 2001; Malhi *et al.*, 2004). After estimating C from AGLB using biomass model by Chave *et al.*, it was measured in mega-grams per hectare (Mg ha^{-1}).

Table 1. Overall mean estimates of C stocks for the study area measured in Mg ha^{-1} with Standard Deviations (SD) in parenthesis

AGB Component for 2009 estimates	Yalu lowland Forest (both PF and SF)	Gabensis lowland Forest (mostly PF)
$AGLB_{DBH>10cm}$	110.19 *(27.58)*	119.21 *(37.19)*
Est._ $AGLB_{DBH<10cm}$	11.02	11.92
Total AGLB	**121.21***(70.12)*	**131.13***(75.87)*
Sample Size (*n*=18)	16	2
AGB Component for 2014 estimates	Oomsis upland Forest (mostly SF)	Yalu upland Forest (both PF and SF)
$AGLB_{DBH>10cm}$	84.2 *(17.43)*	126.06 *(77.35)*

Est._AGLB$_{DBH<10cm}$	8.42	12.61
Total AGLB	**92.62**(*53.58*)	**138.67**(*80.22*)
Sample Size (*n*=14)	6	8

PF: Primary Forest; SF: Secondary Forest (Note: AGLB$_{DBH>10cm}$ was the primary measurement thusEst._AGLB$_{DBH<10cm}$ denotes that AGLB$_{DBH<10cm}$ was estimated.

Table 1 shows the overall mean estimates of C stocks for the two major AGB components (Gibs*et et al*., 2007) in each temporal ground estimates over the sampled sites of the study area measured in Mg ha^{-1}with standard deviations of the measured component (i.e. AGLB$_{DBH>10cm}$) and the total AGLB in parenthesis (Yosi, 2011). This study limited the estimation of C stocks solely on the AGLB component of the AGB excluding the NLB (non-living biomass) component which comprises fine litter (FL) and coarse woody debris (CWD) (Fox *et al*., 2010; Yosi, 2011)that accumulates on forest floors.From Table 1 the *C* measure of AGLB$_{DBH<10cm}$ was estimated with a compromised factor of 10% of AGLB$_{DBH>10cm}$ for both 2009 and 2014 estimates according to the proportionality of PF and SF by each temporal estimate. These factors for AGLB$_{DBH<10cm}$ estimation were derived from Fox *et al.* (2010).C estimates of total AGLB given here are comparable to those given in Fox *et al*. (2010& 2011a). However, this study predicated the average measure on the coupling of both stratums (PF & SF).

The entire ground estimate was divided into training dataset and validation dataset in which all sampled data from the sample sites presented in Table 1 were used as the training dataset and only the sample data from Gabensis (*n*=2) (Yosi, 2011) were withheld as the validation dataset. In addition to the validation dataset, sample data from two 1 ha PSPs in Yalu having 6 samples each were included.

3.2 *Satellite Data Preprocessing and Collateral Data*

Two Optical RapidEye satellite imageries for 2010 and 2014 were obtained and used in this study. These two RapidEye imageries are 5-band multi-spectral (Blue, Green, Red, Red Edge and NIR-Near infrared) image data acquired at a spatial resolution (pixel accuracy) of 5 meters and orthorectified at processing level 3A. Geo-referencing was done at an accuracy of 12.7m(CE90) on a map scale of 1:25,000. The projection system used was Universal Transverse Mercator (UTM), Zone 55 South on World Grid System 1984 (WGS84) Datum in metric units.

Final preprocessing included atmospheric correction for reduction of haze and also other influences of atmospheric and solar illumination (Eckert, 2012).Prior to the final preprocessing, the RapidEye imageries were subsetted using a vector mask to delineate the boundary of Wampar LLG producing the cropped scene of the study area. Finally, in their given order above, the RapidEye imageries were integrated with the 2009 and 2014 ground estimates (of AGB and C) respectively to produce spatially distributed estimations for the low-altitude forest landscape studied.

A forest-base land cover/use map for 2012 was derived from the combination of opticalRapidEye imageries and Radar (ALOS – PALSAR) satellite data with existing forest-base data under the JICA – PNGFA Project, which was initiated in 2011 (The National, 2014, March 13). This Forest-base Map comprised all identified forest stratums by the PNGFRI with other momentousagriculture and forestry land-uses and was produced at national and provincial levels. The subset for the study area (Figure 2) was retrieved from the provincial level Forest-base Map and is presented at a map scale of 1:150,000 showing terrain of hill-shading derived from a 30m Digital Elevation Model (DEM). Current active forestry activity or land-use within the study area illustrated in Figure 2is the Morobe Concession area coded as a forest mapping unit 1201 (Mor_con_1201_FMU) and the Oomsis Pine Plantation. This

Forest-base Map for the study area was the collateral data used to evaluate the two broad forest stratums studied.
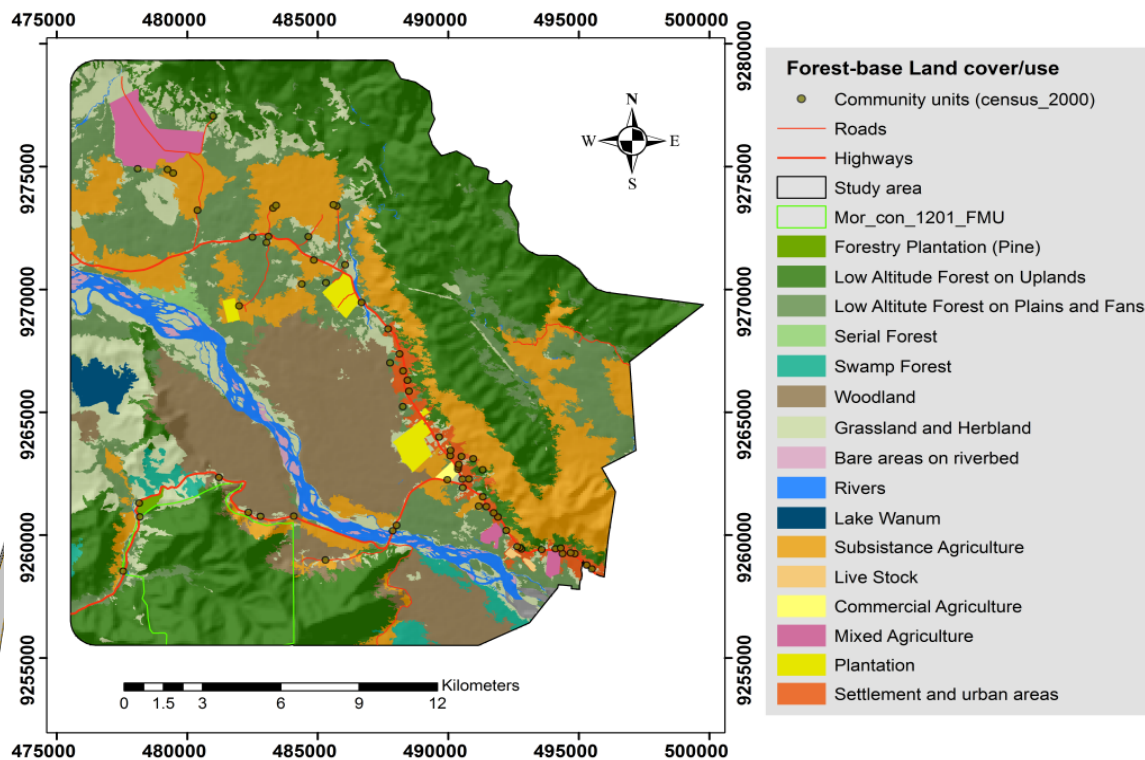

Fig 2. Forest-base map for the study area generated from Morobe Forest-base Map 2012.

3.3 *Spectral Vegetation Indices, Image Transforms and Simple Reflectance*

Following the preprocessing of the RapidEye satellite data, a number of specific spectral indices were generated from image spectral bands by either vegetation index or simple ratio index. Simple band rationing involved single bands in each ratio component whereas vegetation indices utilised multiple bands being inputted in each of the ratio components (see Table 2) and were categorised into traditional and complex (Wijaya *et al*., 2010a). Since the Rapid Eye imageries consist of a narrow-band, that is, the Red Edge Band, all spectral indices generated using the Red Band were also generated using the Red Edge Band. Red Edge-derived spectral indices acted as an added set of variables to the overall estimation process. Moreover, unlike previous studies in which narrow-band (Red Edge) indices were limited to traditional Normalised Differential Vegetation Index (NDVI) and Ratio Vegetation Index (RVI) with certain specificity (Sims *et al*., 2002; Datt, 1999), this study presents an exploratory trend of generating all possible indices from the Red Edge narrow-band that are normally generated using the Red Band specifically to test for significance in correlation with AGB and C. Detailed descriptions on the utility of and further information about the spectral vegetation indices used here can be found in the respective sources cited (Table 2). Apart from spectral indices, the spectral image transforms of Principal Component Analysis (PCA) was conducted to extract components according to the number of RapidEye bands. Additionally, single spectral bands of the RapidEye imageries were also extracted and Table 2 shows a list of all the spectral parameters tested.

Table 2. Various spectral parameters such as single image bands, image transforms, simple band ratio indices, traditional vegetation indices and complex vegetation indices generated and tested for variable appropriation for the AGB and C modelling.

Spectral parameter	Formula	Reference
Single image bands (RapidEyebands 1 – 5)		
Simple Band Ratio: RVI (RVI_re) NIR/Green GRVI (GRVI_re)	NIR/Red $NIR/Green$ $Green/Red$	(Jordan, 1969) (Eckert, 2012) (Kanemasu, 1974)
Image Transform (PCA1-PCA5)		(Wijaya *et al.*, 2010a&b and Eckert, 2012)
Traditional Vegetation Index: NDVI (NDVI_re) ND32 (ND42_re)	$(NIR–Red)/(NIR + Red)$ $(Red – Green)/(Red + Green)$	(Rouse *et al.*, 1973)
Complex Vegetation Index: EVI (EVI_re)	$2.5 \times (NIR–Red)/(NIR – 6Red – 7.5Blue + 1)$	(Huete *et al.*, 1997)
SAVI (SAVI_re)	$(NIR–RED)\times(1 + L)/(NIR+RED+ L)$	(Huete, 1988)
MSAVI (MSAVI_re)	$\left[(2NIR+1)-\sqrt{(2NIR+1)^2-8(NIR-2RED)}\right]/2$	(Qi *et al.*, 1994a&b)
GEMI (GEMI_re)	$\varepsilon(1-0.25\varepsilon)-(Red–0.125)/(1–Red)$ where $\varepsilon = (2(NIR^2–Red^2)+1.5NIR+0.5Red)/(NIR+Red+0.5)$	(Pinty and Verstraete, 1991)

GRVI: green ratio vegetation index; ND32; NDVI using the 3rd band (red) and the 2nd band (green); EVI: Enhanced Vegetation Index; SAVI: soil-adjusted vegetation index, L= 0.5; MSAVI: attuned modified soil-adjusted vegetation index; GEMI: Global Environmental Vegetation Index(Note: for every "_re" specified index for example, "NDVI_re" denotes that a Red Edge index was calculated for the particular type of index simply by substituting every Red band input with Red Edge Band. Also, ND42_re denotes NDVI using the 4th band (Red Edge) with the 2nd band).

3.4 Statistical Analysis

Training datasets for 2009 ground estimates were 16 plots while those for 2014 were 14 plots. These training datasets were used to extract pixel values from the generated spectral parameters using on-ground plot locations. To analyse the relationships of AGB and C with values extracted from the spectral parameters, Pearson's Correlation was used to correlate AGB and C with each of these spectral parameters to determine appropriate predictor variables for modeling and estimation. Only highly correlated spectral parameters were selected as preeminent predictor variables and were used in a Geographic Information System(GIS) environment to conduct a Spatial Ordinary Least Square (OLS) Regression Analysis (Longley *et al.*, 2005) to generate estimation models for C stocks. The

spatial linear OLS regression was performed in a step-wise approach (Eckert, 2012; Wijaya *et al.*, 2010a). Stratum-specific modeling was conducted in which the training datasets from each ground estimate plotted on each corresponding temporal image data (i.e. 2009 estimates on 2010 image and 2014 estimates on 2014 image) were divided into PF and SF identifiably for each temporal estimate and modeled correspondingly. Since stratum-specific samples were rather small, individual models were developed for only single preeminent predictor variables and a combination through model-fitting was done to produce an overall estimation trend for each temporal estimate. The coefficient of determinant R^2, its reliable counterpart adjusted R^2 and model probability(p-level) were the relevant statistical parameters used to assess model performance and model-fits in each forest stratum. Robust spatial statistical probabilities namely, Joint F-Statistic and Joint Wald Statistic were also taken into account to primarily assess overall model significance while Jarque-Bera statistic primarily assessed model bias. Finally, Spatial Autocorrelation (Moran's Index) (Longley *et al.*, 2005) was used to assess residual spatial autocorrelation on each OLS regression model to ensure that their residuals were randomly distributed.

Plot-level model validation was done utilising the withheld validation dataset with model-fitted preeminent predictor variables calculating their resultant root mean square error (RMSE) and variance ratio (VR) (Muukkonen and Heiskanen, 2006; Powel *et al.*, 2010; Wijaya *et al.*, 2010b).VR and RMSE with the relative counterpart of the latter which is RMSE, (Muukkonen andHeiskanen, 2006;Wijaya*et al.*, 2010b)were directly applied to individual models for PF and SF and their subsequent model-fits as secondary measures to assess model performance and significance.

4. Results and Discussions

4.1Correlation of Spectral parameters with AGB and C

Pearson's correlation identified highly correlated variables (spectral parameters) with AGB and C prior tomodeling; thus, for PF and SF in 2010spectral imageries, the preeminent single index variables identified were NDVI with $R^2 = 0.808$ ($p = 0.006$) and GRVI with $R^2 = 0.669$ ($p = 0.007$) respectively. For the 2014 spectral imageries, the preeminent index variables identified were GRVI_re with$R^2 = 0.817$ ($p = 0.011$)for PF and RVI_re with$R^2 = 0.52$ ($p = 0.043$) for SF. Since the level of correlation was quite high, only high correlations of Pearson's Coefficient 'r' = > 0.7 with associated linearR^2andsignificant p-levels are listed in Table 3.

Table 3. Tested spectral variables and stratum-specific preeminent single variables (bolded) listed with statistically significant Pearson's correlation coefficients r, p-levels and linear$R^2$for linear relationships with AGB and C

Stratum	Spectral parameter	Pearson's r	R^2
PF_RE_2010 (*n*=7)	NIR Band	0.728	0.529
	NIR/Green	0.862(*)	0.743
	RVI	0.883(**)	0.780
	GRVI_re	-0.872(*)	0.760
	NDVI	**0.899(**)**	**0.808**
	ND42_re	0.871(*)	0.757
	PCA1	0.806(*)	0.649
	PCA2	-0.896(**)	0.802
	EVI	-0.896(**)	0.803
	EVI_re	-0.881(**)	0.776

	SAVI	0.887(**)	0.786
	MSAVI	0.886(**)	0.784
	GEMI	-0.880(**)	0.774
	GEMI_re	-0.890(**)	0.792
SF_RE_2010 (*n*=9)	RVI	0.756(*)	0.572
	GRVI	**0.818(**)**	**0.669**
	EVI	-0.741(*)	0.549
	EVI_re	-0.719(*)	0.517
	SAVI	0.740(*)	0.699
	MSAVI	0.734(*)	0.539
	GEMI_re	-0.701(*)	0.491
2009 Field data (total *n*=16)			
PF_RE_2014 (*n*=6)	NIR/Green	-0.760(*)	0.577
	GRVI_re	**0.904(*)**	**0.817**
	PCA5	0.702	0.493
SF_RE_2014 (*n*=8)	**RVI_re**	**0.721(*)**	**0.520**
	MSAVI_re	0.709(*)	0.503
2014 Field data (total *n*=14)			

Code example - PF_RE_: PF on RapidEye temporal image;(**) significant correlation at 0.01 level and (*) significant correlation at 0.05 level.

Most of the statistically significant spectral parameters for PF_RE_2010 were at a p-level of<0.01 including the preeminent variable NDVI while the single spectral band NIR had a good correlation (R^2 = 0.529) but a very poor p-value of 5.661. SF_RE_2014 had only the preeminent variable GRVI with statistical significance at p-level< 0.01. All parameters for both stratums in the 2014 image including their respective preeminent variables had p-levels < 0.05 while only PCA5 under PF_RE_2014 had an insignificant p-value of 0.446 although it had a substantially good correlation.

4.2 *Spatial Ordinary Least Square (OLS) Regression Analysis*

Spatial Ordinary Least Square (OLS) Regression Models were developed on a stratum-specific basis where AGB/C was the dependent variable and a single preeminent spectral parameter was used as the predictor variable. As assumed, the selected preeminent spectral parameters produced spatially and statistically significant models given in Table 4 with certain relevant spatial statistical parameters.

Table 4. Relevant statistics for the developed stratum-specific models for 2010 and 2014 with their model-fits

Model stratum	R^2	Adj. R^2	VR	RMSE (AGB) [Mg ha^{-1}]	RMSE (C) [Mg ha^{-1}]	RMSE$_r$ (C) [%]	Joint F-Statistic (p-value)	Joint Wald Statistic (p-value)
PF10_NDVI (n = 7)	0.808	0.770	0.899	8.544	4.272	3.077	0.005909	0.000000
SF10_GRVI (n = 9)	0.669	0.622	0.818	16.040	8.020	8.894	0.007058	0.000429
Model-fit (n = 16) PF&SF_10	**0.739**	**0.696**	**0.969**	**13.290**	**6.646**	**5.963**		
PF14_GRVI_re (n = 6)	0.817	0.772	0.904	56.624	28.312	21.132	0.013365	0.000001
SF14_RVI_re (n = 8)	0.520	0.440	0.721	18.010	9.005	11.292	0.043406	0.000952
Model-fit (n = 14) PF&SF_14	**0.669**	**0.606**	**0.925**	**34.982**	**17.491**	**16.984**		

Code example, (a) PF10_NDVI: 2010 PF model using preeminent variable NDVI; (b) PF&SF_14: combined model-fit for 2014.

The models developed for 2010 PF and SF had more satisfying spatial statistical probabilities(Joint F-statistic & Joint Wald Statistic) at p-levels< 0.01 and< 0.001 (Table 4) respectively in which a relevant p-value of Joint F-statistic assumes an overall model significance while a relevant p-value of Joint Wald Statistic indicates robust overall model significance. Concerning the model complexities, the 2010 models showed significant measures of adjusted R^2 that explained 77% of the variation of AGB and C in PF and 62.2% of the variation of AGB and C in SF. Consequently, the PF model achieved a C relative RMSE of 3.08% corresponding to a RMSE of 4.27MgCha^{-1}and 8.54MgAGBha^{-1}while the SF model achieved a C relative RMSE of 8.89% with corresponding RMSE of 8.02MgCha^{-1}and 16.04MgAGBha^{-1}. Model-fitting of these two models for 2010 achieved a combined mean adjusted R^2 attuned to a value of 0.696. The attuned C relative RMSE for the model-fit was 5.96% with a corresponding RMSE of 6.65MgCha^{-1}and 13.29MgAGBha^{-1} showing a good adjustment to fit both models. For 2014, the Joint F-statistic and Joint Wald Statistic were significant at p-levels < 0.05 and < 0.001 respectively for both PF and SF. The PF model for 2014 had a significant adjusted R^2 that explained 77.2% of variation in AGB and C (similar to 2010 PF model),whereas the SF model had also a considerably significant adjusted R^2 explaining 44% of AGB and C variation. Having quite a high corresponding RMSE of 28.31MgCha^{-1}and 56.62MgAGBha^{-1}, the C relative RMSE for the 2014 PF model was 21.13% while the SF model had a C relative RMSE of 11.29% with corresponding RMSE of 9MgCha^{-1}and 18MgAGBha^{-1}. Combining these two 2014 models in a model-fit, the adjusted $R^2$was attuned by averaging to 0.606 with also an attuned C relative RMSE of 16.98% corresponding to a RMSE of 17.49MgCha^{-1}and 34.982MgAGBha^{-1} that also suites the fit of both models.

Figure 3 shows the relationship between measured and estimated C stocks for the stratum-specific models for 2010 and 2014 plotted in a model-fit. It also shows the spatially distributed

temporal C stock maps (being measured according to modeled estimates) of a scene where Yalu plots are located (refer to Figure 1). Obviously, the model-fits show the entire sample plots for each year graphically through combining the stratum-specific models. It is impressing to note that stratum-specific models for 2010 were both at 99% confidence interval ($p< 0.01$) while those for 2014 were also both significant at 95% confidence interval ($p< 0.05$). Regarding overestimation and underestimation, the overall highest and lowest measured C in 2009 (for 2010 image) were 152.828Mg ha^{-1} and 77.405Mg ha^{-1} respectively and interestingly the highest measured C was not much underestimated given an estimate of 152.228Mg ha^{-1} with similar reduced overestimation of the lowest measured C to 78.693Mg ha^{-1}. The overall highest and lowest measured C in 2014 (for 2014 image) were 281.369Mg ha^{-1} and 52.147Mg ha^{-1} respectively and were underestimated to 250.178Mg ha^{-1} and overestimated to 71.365Mg ha^{-1} in that order.
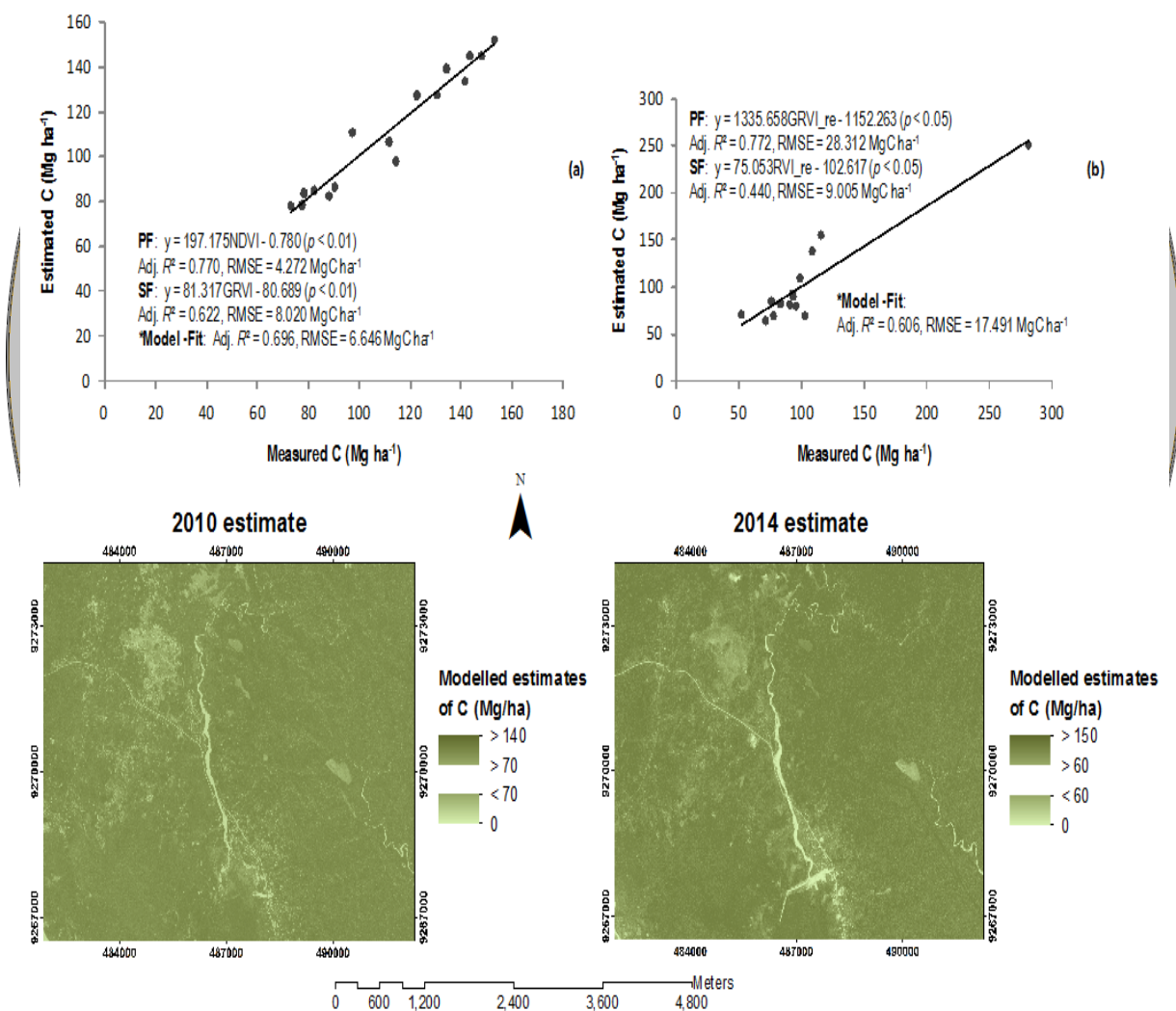
Fig 3. Model-fits for the developed PF and SF models for 2010 (a) and 2014 (b) with subsequent spatially distributed scene-level C stock maps

4.3 *Discussion*

The high spatial resolution (5m) of the RapidEye imageries provided a robust capture of the forest,which was advantageous for linking of ground estimates of AGB and C. Forest inventories in this study were designed to cover the major stratums across the low-altitude landscape of the study area taking samples in both lowlands and uplands. As ground-truthing, forest inventories proved the different levels of forest disturbance (land-cover/use) depicted by the Forest-base Map in Figure 2and how these disturbances affected AGB and C estimates at plot levels and even spatial levels. These disturbances comprised the different types of land-use activities that affected the C content of the study area. The Forest-base Map also provided a standard classification of forest stratums that aided in defining the two broad stratums analysed in this study and also provided an insight on how C is spatially distributed among these forest stratums. Also, respective of the Forest-base Map, the forest stratums sampled and analysed included the three major stratums which are low-altitude forest on uplands, low-altitude forest on plains and fans and woodland (refer to Figure 2).

Spectral indices derived from Red Edge band were generated on an explorative basis and incorporated as added variables to test for significance of correlation with AGB and C. It was discovered by Pearson's correlation that (i) the added variables of Red Edge-derived spectral indices had overall high significance when correlated with AGB and C, (ii) Red Edge-derived spectral indices also evinced better correlations with 2014 ground estimates of AGB and C when normal Red-derived spectral indices had few significant correlations or even failed to correlate at all and (iii) all significant spectral variables had stronger correlations with AGB and C in PF than in SF. Evaluating the significant spectral parameters presented in Table 3, Red Edge derived spectral indices were very helpful and had momentous confidence levels and strong correlation with AGB and C overall and were very pertinent variables in 2014.

Spatial OLS regression models were developed on a stratum-specific premise to estimate AGB and C of PF and SF and then integrated to produce a spatially resolved model-fit composite for each temporal landscape. The model-fit essentially shows the relationship between the estimated and measured C stocks for the entire sample in each temporal estimate (Figure 3). The idea of model-fitting in this study does not necessarily signify that the fitting will develop an integrated model for AGB and C estimation across the study area for both PF and SF because individual model performance will vary causing unreliable estimation unless multiple variables are used to develop the model as shown in Wijaya *et al*. (2010) or Eckert (2012); thus, there were no spatial statistics for the model-fits. It, however, focuses on validating the fitting process in the spatial domain where modeled outputs from each stratum-specific model recombined by an intersecting overlay process to produce a single integrated composite that still retains the individual model performance of each stratum-specific model. Resultantly, this single integrated composite is the spatially resolved C stock map for each temporal estimate that provides a measure of these modeled estimates and the unestimated category as well. Moreover, the lowest measurement of the C stock maps were zero indicating non-forest areas with exposed soil whereas according to spectral vegetation indices the lowest values are negative values indicating water bodies and the exemplified water bodies in these modeled spectral indices outputs are the two small rivers depicted in the maps in Figure 3.

Adjusted R^2 values of both model-fits for the temporal estimates were attuned to satisfiable values which are 0.696 for 2010 and 0.606 for 2014 (Table 4). The reason for averaging the adjusted R^2 values of the stratum-specific models in each temporal estimate to come up with the adjusted R^2 values for the model-fits was because the spatial integration of the stratum-specific

modeled outputs as elucidated enabled individual models within the integrated composite to maintain independent significant relationships with C stocks. As a result, the mean adjusted R^2 for the model-fits are relevantly suitable for both model complexities across each temporal landscape explaining respective variations in C stocks. VR (variance ratio) is expressed according to Powel *et al*. (2010) as the standard deviation of the measured (observed) C divided by the standard deviation of the modeled (estimated) C. All VRs calculated in this study (Table 4) to assess model performance and significance of stratum-specific models and model-fits in terms of C stock variance were relevant when compared with values obtained in Powel *et al*. (2010). Most importantly, the corresponding attuned RMSEs and relative RMSEs of the model-fits evinced values that suited both stratum-specific models in each temporal landscape which directly implied a validation of the fitting. Overall RMSEs for all models in both temporal estimates were reasonably low with values < 9MgC ha^{-1} (8.02MgC ha^{-1}) and < 29MgC ha^{-1}(28.31MgC ha^{-1}). The C relative RMSE of each stratum-specific model in each temporal estimate were relevantly low except for the PF model in 2014 which had a C relative RMSE> 20% (21.13%).

With reference to model estimation, 2010 models had high confidence levels ($p< 0.01$) so their performances were complacent in terms of over- and underestimations while 2014 models had at least reasonable over- and underestimations according to their sound confidence levels ($p< 0.05$). Mean measured estimate with standard deviations of both stratums in 2009 was 111.4531±27.968MgC ha^{-1} and mean modeled (2010) estimate was 111.4529±27.113MgC ha^{-1} owed to the 99% ($p< 0.01$) confidence intervals of both models and individual model performances. Those for 2014 were 102.9857±53.897MgC ha^{-1}(measured) and 102.9857±851MgC ha^{-1}(modeled) also having much influence from individual model performances and the respective 95% ($p< 0.05$) confidence intervals for both stratum-specific models. To note, the estimated AGB and C for SF in this study may not be representative of the disturbed SF across PNG because such forests have undergone intensive selective-logging where larger trees with DBH > 50cm have been removed for timber. C stock variation and saturation in each temporal C stock map reflected the modeled capture of each preeminent spectral index and the C stock maps also depicted how certain forest disturbances affected the C content across each temporal landscape.

Concerning critical issues, although the sample sizes of measured AGB and C were critically small, the notion of stratum-specific modeling and subsequent model-fitting provided convenience for reliable estimation with such small samples. Unlike Eckert's (2012) study where bootstrapping was used to increase sample sizes (n) for stratum-specific modeling, the approach here is directly stratum-specific in which the limited samples were separated into PF and SF accordingly and appreciably correlations were quite high (see Table 3) despite the small sample sizes. On a spatial platform in remote sensing context, stratum-specific models will have certain redundancies since a generic satellite image captures a combined variation of different forest stratums which appear homogeneous. Therefore, defining broad forest stratums before stratum-specific modeling was a critical consideration in this study and model-fitting in terms of overlaying stratum-specific modeled outputs was the key solution to this drawback of remote sensing redundancies. Moreover, the output model-fitted composites were the results of spatial overlaying with the allowance of temporal landscape intersection that drastically minimizes these redundancies while enhancing the spatial distribution of C estimates.

Since, Joint F-Statistic and Joint Wald Statistic showed high spatial statistical significance with relevant confidence levels ($p< 0.05$ and $p< 0.001$ respectively); the Jarque-Bera statistic was

used to assess model bias in terms of skewness for each developed model assuming that their residuals were not normally distributed. A significant Jarque-Bera p-value of < 0.05 or 95% confidence interval indicates that the model is biased therefore, reporting with direct reference to the order of the stratum-specific models given in Table 4 (excluding model-fits), Jarque-Bera p-values were 0.842, 0.932, 0.713 and 0.459, assuming random distribution of the model residuals. An added spatial statistical evaluation of model residuals involved the processing of the stratum-specific regression models using Spatial Autocorrelation via Global Moran's Index with the same assumption as that of Jarque-Bera statistic except that in this evaluation, model residuals were assessed for 'spatially' random distribution. Following the order of Jarque-Bera p-values for stratum-specific models, Spatial Autocorrelation p-values were 0.324, 0.105, 0.630 and 0.413, signifying that the residuals of the stratum-specific regression models are spatially random.

Finally, the concept of stratum-specific modeling presented here can be verified by application in further studies at regional (provincial) and national levels conveniently using PSP data on medium to moderate resolution satellite data such as Landsat 7 ETM+ data and MODIS (Moderate resolution Imaging Spectroradiometer) data respectively.

5. Conclusion

Interesting relationships were discovered in the process of integrating ground estimates of AGB and C with the RapidEye data by studying these relationships via Pearson's correlation and developing appropriate models through the spatial OLS regression analysis. Generally assessing confidence levels (p-levels), through correlation significance and statistical variable significance, Red Edge-derived spectral indices showed robust performances and truly acted as an added (enhanced) set of variables to cater for failed correlations of AGB and C with indices usually derived from Red band. This therefore, confirmed acceptance of the hypothesis of the Red Edge band posed earlier in this paper. High confidence levels in both temporal estimates at 99% and 95% confidence levels for 2010 and 2014 respectively with significant model complexity measures(adjusted R^2) and low RMSEs and relative RMSEs were statistical proofs that the stratum-specific models developed are reliable in estimating AGB and C. Furthermore, the notion of model-fitting relevantly showed the combined importance of the stratum-specific models for each temporal estimate exposing all sample plots graphically and importantly, validating the integration of these models in the spatial domain with significantly attuned RMSEs and relative RMSEs. Consequently, spatial level estimation via the intersecting overlay process is now a reliable approach of producing spatially distributed estimates for the entire landscape studied. This also proves acceptance of the idea hypothesized for this strategy of model-fitting. Finally, from deductive reasoning of the results obtained in this study with reflection to forest C stocks from the overall measured low-altitude tree species including those common in the PSPs across PNG and also having comparable ground estimates with previous national level studies namely, Fox *et al*. (2010 and 2011a) and Yosi (2011), the concept of stratum-specific modeling presented here can be significantly tested or applied in other low-altitude forest landscapes in PNG with high resolution optical satellite data for AGB and C estimation at spatial levels for REDD+ implementations.

6. Acknowledgment

7. References

1. Brown, S. & Lugo, A. E. (1990). Tropical secondary forests. *Journal of Tropical Ecology,* 6, 1-32.
2. Brown, S. (1997). Estimating biomass and biomass change of tropical forests: a primer. In FAO Forestry Paper, 134; 55.Rome, Italy, FAO.
3. Bryan, J., Shearman, P., Ash, J. &Kirkpatrick, J. B. (2010). On estimating tropical forest carbon dynamics in Papua New Guinea.*Annals of Forest Science*. [doi: 10.1007/s13595-011-0042-x]
4. Chave, J., Condit, R., Lao, S., Caspersen, J. P., Foster, R. B. and Hubbell, S. P., (2003), Spatial and temporal variation of biomass in a tropical forest: results from a 20 large census plot in Panama, *Journal of Ecology,* 91, 240-252.
5. Chave, J., Andalo, C., Brown, S., Cairns, M. A., Chambers, J. Q., Eamus, D., Fölster, H., Fromard, F., Higuchi, N., Kira, T., Lescure, J. P., Puig, H., Riéra, B. & Yamakura, T., (2005), Tree allometry and improved estimation of carbon stocks and balance in tropical forests, *Oecologia,* 145, 87-99.
6. Clark, D. A., Brown, S.,Kicklighter, D. W., Chambers, J. Q., Thomlinson, J. R., Ni, J., and Holland, E. A., (2001), Net primary productionin tropical forests: An evaluation and synthesis of existing field data, *Ecol. Appl.,* 11: 371–384.
7. Datt, B., (1999), A New Reflectance Index for Remote Sensing of Chlorophyll Content in Higher Plants: Tests Using Eucalyptus Leaves, *Journal of Plant Physiology,* 154:30-36.
8. Eckert, S., (2012), Improved Forest Biomass and Carbon Estimations Using Texture Measures from World-View2 Satellite Data, *Remote Sens.,* 4, 810-829 [doi:10.3390/rs4040810].
9. Eddowes, P. J., (1977), Commercial timbers of Papua New Guinea; their properties and uses.Office of Forests, Papua New Guinea, PortMoresby.
10. Fox, J. C., Yosi, C. K., Nimiago, P., Oavika, F., Pokana, N., Layong, K., & Keenan, R. J., (2010), Assessment of Aboveground Carbon in Primary and Selectively Harvested Tropical Forest in Papua New Guinea, *Biotropica,* 42(4): 410–419 [doi:10.1111/j.1744-7429.2009.00617.x].
11. Fox, J. C., Vieilledent, G., Yosi, C. K., Pokana J. N., & Keenan R., J., (2011a), Aboveground Forest Carbon Dynamics in Papua New Guinea: Isolating the Influence of Selective-Harvesting and El Niño. *Ecosystems* 14:1276-1288 ISSN 1432-9840 [doi:10.1007/s10021-011-9480-4].
12. Fox, J. C., Yosi, C. K.&Keenan, R. J., (2011b), Assessment of timber and carbon stocks for community forest management.InFox, J. C., Keenan, R. J., Brack, C. L. &Saulei, S. (eds.), *Native forest management in Papua New Guinea: advances in assessment, modelling, and*

*decision-making,*ACIAR ProceedingNo. 135, 42-52. Canberra: Australian Centre for International Agricultural Research.

13. Gibbs, H. K., Brown, S., Niles, J. O. & Foley, J. A., (2007), Monitoring and estimating tropical forest carbon stocks: making REDD a reality, *Environ. Res. Lett.,* 2, 045023 [doi:10.1088/17489326/2/4/045023].

14. Hall, R. J., Skakun, R. S., Arsenault, E. J., and Case, B. S., (2006), Modelling forest stand structure attributes using Landsat ETM+ data: Application to mapping of aboveground biomass and stand volume, *Forest Ecology and Management,* 225,378−390

15. Houghton, R. A., Lawrence, K. T., Hackler, J. L. and Brown, S., (2001), The spatial distribution of forest biomass in the Brazilian Amazon: A comparison of estimates, *Glob. Change Biol.,* 7, 731–746.

16. Huete, A. R., (1988), A Soil-Adjusted Vegetation Index (SAVI), *Remote Sensing of Environment,* 25, 295-309.

17. IPCC,(2006). 2006 IPCC guidelines for National Greenhouse Gas Inventories, prepared by the National Greenhouse Gas Inventories Programme.InH. S. Eggleston, L.Buendia, K. Miwa, T. Ngara, and K. Tanabe (Eds), *IGES,* Japan.

18. Jordan, C. F., (1969), Derivation of leaf area index from quality of light on the floor, *Ecology,* 50, 663-666.

19. Kanemasu, E. T., (1974), Seasonal canopy reflectance patterns of wheat, sorghum, and soybean, *RemoteSens. Environ.,* 3, 43-47.

20. Longley, P. A., Goodchild, M. F., Maguire D. J. and Rhind, D. W., (2005), Geographical Information Systems and Science (2nd Ed.).John Wiley & Sons Ltd.The Atrium, Southern Gate, Chichester, West Sussex PO19 8SQ, England.

21. Malhi, Y., Baker, T. R., Phillips, O. L., Almeida, S.,Alvarez, E., Arroyo, L., Chave, J., Czimczik, C. I., Di Fiore, A.,Higuchi, N., Killeen, T. J., Laurance, S. G., Laurance, W. F., Lewis, S. L., Montoya, L. M. M.,Monteagudo, A., Neill, D. A., Vargas, P.N.,Patino, S., Pitman, N. C. A., Quesada, C. A., Salomao, R., Silva, J. N. M.,Lezama, A. T., Martinez, R. V.,Terborgh, J.,Vinceti, B., and Lloyd, J., (2004), The abovegroundcoarse wood productivity of 104 Neotropical forest plots,*Glob. Change Biol.,* 10, 563–591.

22. Muukkonen, P. and Heiskanen, J., (2006), Biomass estimation over a large area based on stand-wise forest inventory data and ASTER and MODIS satellite data: A possibility to verify carbon inventories, *Remote Sensing of Environment,* 107, 617–624.

23. Pinty, B. and Verstraete, M. M., (1991), GEMI: a non-linear index to monitor global vegetation from satellites, *Vegetation*, 101, 15–20.

24. Powell, S. L., Cohen, W. B., Healey, S. P., Kennedy, R. E., Moisen, G. G., Pierce, K. B., and Ohmann, J. L., (2010), Quantification of live aboveground forest biomass dynamics with Landsat time-series and field inventory data: A comparison of empirical modeling approaches. *Remote Sensing of Environment,* 114, 1053–1068.

25. Qi J., Chehbouni A., Huete A.R., Kerr Y.H., 1994. Modified Soil Adjusted Vegetation Index (MSAVI). *Remote Sens Environ* 48:119-126.

26. Rahman, M. M., Csaplovics, E., & Koch, B., (2008), Satellite estimation of forest carbon using regression models, *International Journal of Remote Sensing*, 29, 6917−6936.

27. Rosenqvist, A., Shimada, M., Ito, N. and Watanabe, M., (2007), ALOS PALSAR: A Pathfinder Mission for Global-Scale Monitoring of the Environment. *IEEE TRANSACTIONS ON GEOSCIENCE AND REMOTE SENSING*, 45(11), 3307-3316 [doi:10.1109/TGRS.2007.901027]

28. Rouse, J.W., Haas, R.H., Schell, J.A., Deering,and D.W., (1973), Monitoring vegetation systems in the Great Plains with ERTS. In *Third ERTS Symposium, NASASP-351 I,* I, 309–317.

29. Shearman, P. L., Bryan, J. E., Ash J., Hunnam. P., Mackey, B., Lokes, B., (2008), The state of the forests of Papua New Guinea.Mappingthe extent and condition of forest cover and measuring thedrivers of forest change in the period 1972–2002.University of Papua New Guinea.

30. Sims, D. A. and Gamon, J. A., (2002), Relationships between leaf pigment content and spectral reflectance across a wide range of species, leaf structures and developmental stages, *Remote Sensing of Environment,* 81, 337-354.

31. Singh, M., Malhi, Y., and Bhagwat, S., (2014*),* Evaluating land use and aboveground biomass dynamics in an oil palm–dominated landscape in Borneo using optical remote sensing, *Journal of Applied Remote Sensing,* 8(1) article 083695 [doi:10.1117/1.JRS.8.083695].

32. The National, (2014-March 13), JICA-PNGFA PROJECT Capacity Development on Forest Monitoring for AddressingClimate Change.*National Supplement*, pp. 28-29. Retrieved from: http://www.jica.go.jp/png/english/office/topics/c8h0vm00008p9s0c-att/140313.pdf

33. UNFCCC (United Nations framework Convention on Climate Change), (2009), Report on the expert meeting on methodological issues relating to reference emission levels and reference levels. Subsidiary body for scientific and technological advice.Thirtieth session. Bonn, 1–10 June 2009. FCCC/SBSTA/2009/2. 14 May 2009.

34. UNFCCC (United Nations framework Convention on Climate Change) (2010). Draft decision CP/16, Outcome of the work of the ad hoc working group on long-term cooperative action under the convention, UNFCCC, Bonn, Germany. Available from: http://unfccc.int/files/meetings/cop_16/application/pdf/cop16_lca.pdf.

35. Wijaya, A., Kusandi, S., Gloaguen, R. &Heilmeier, H., (2010a), Improved strategy for estimating stem volume and forest biomass using moderate resolution remote sensing data and GIS, *Journal of Forestry Research,* 21(1), 1–12 [doi: 10.1007/s11676-010-0001-7].

36. Wijaya, A., Leisenberg, B. andGloaguen, R., (2010b), Retrieval of forest attributes in complex successional forests of Central Indonesia: Modelling and estimation of bitemporal data, *Forest Ecology and Management,* 259, 2315–2326.

37. Yali, G. and Samanta, S., (2014), Biomass and Carbon Stock Estimation using High Spatial Resolution Satellite Data, *Journal of Environmental Research and Development,* 8(3A).

38. Yosi, C. K., (2011), Scenarios for community-based management of cutover native forest in Papua New Guinea. PhD Thesis. Department of Forest and Ecosystem Science, The University of Melbourne, Australia.

39. Zheng, D., Rademacher, J., Chen, J., Crow, T., Bresee, M., Le Moine, J., (2004), Estimating aboveground biomass using Landsat ETM+data across a managed landscape in northern Wisconsin, USA, *Remote Sensing of Environment,* 93, 402−411.

Author Biographies

First Author *(corresponding author)* is an MPhil Scholar in Geomatics having completed his MPhil at the PNG University of Technology during 2014 - 2015. This paper is a major pre-component of his MPhil research which is on the "assessment of aboveground carbon stocks using Remote Sensing and GIS technologies" in the study area presented here.

Second author (Dr. Sailesh Samanta) is Senior Lecturer and Section Head of GIS section under Department of Surveying and Land Studies at the The Papua New Guinea University of Technology, Papua New Guinea.